Supplementary Material: Density of States of Ru_3 and Pt_3 clusters supported on Sputter-Deposited TiO_2

Liam Howard-Fabretto[1,2], Timothy J. Gorey[3], Guangjing Li[3], Siriluck Tesana[4], Gregory F. Metha[5], Scott L. Anderson[3], and Gunther G. Andersson[1,2]*

1 Flinders Institute for Nanoscale Science and Technology, Flinders University, Adelaide, South Australia 5042, Australia

2 Flinders Microscopy and Microanalysis, College of Science and Engineering, Flinders University, Adelaide, South Australia 5042, Australia

3 Chemistry Department, University of Utah, 315 S. 1400 E., Salt Lake City, UT 84112, United States

4 The MacDiarmid Institute for Advanced Materials and Nanotechnology, School of Physical and Chemical Sciences, University of Canterbury, Christchurch 8141, New Zealand

5 Department of Chemistry, University of Adelaide, Adelaide, South Australia 5005, Australia

*Corresponding author: Gunther G. Andersson

Email: gunther.andersson@flinders.edu.au.

Address: Physical Sciences Building (2111) GPO Box 2100, Adelaide 5001, South Australia

Background

MIES Background

In a UPS measurement, incident ultraviolet (UV) light causes outer valence electrons to be ejected from the sample as photoelectrons due to the photoelectric effect. UPS can be used to measure the electronic properties of a surface such as the occupied density of states (DOS) [1], featuring information depth of ~2-3 nm [2]. Metastable impact electron spectroscopy (MIES) can also be used to measure surface electronic properties such as DOS [3] in a manner similar to UPS. However, rather than firing photons at the surface, metastable helium atoms (He*) with an excitation of 19.8 eV [3] are used which bombard the surface, resulting in a He* de-excitation or neutralisation process and the emission and detection of an electron.

The major advantage of MIES is that it is purely surface sensitive because He* are not able to exceed the Van der Waals interactions at the surface [3, 4], unlike UPS which has an information depth of 2-3 nm [2]. When used together these techniques are complimentary; as an example, a previous study by Chambers *et al.* [5] used UPS and MIES to analyse the valence structure of double-walled carbon nanotubes, and it was shown that UPS measures the DOS across the whole nanotube while MIES only measured the DOS of the outer nanotube layer. However, previous studies using MIES on supported metal clusters are limited. Several MIES studies by Andersson *et al.* [6-8] have been performed on small, TiO_2-supported Au clusters, where the surface sensitivity of MIES was utilised for measuring clusters on the topmost layer.

The mechanism by which an electron is emitted from the surface in MIES is not unique. Electron emissions can occur by two known de-excitation pathways; these are 1) resonance ionisation (RI) followed by Auger neutralisation (AN), and 2) Auger de-excitation (AD) [4, 9]. This has been previously described in detail by Morgner [4]. Any MIES measurement may be some combination of AD and RI+AN to varying degrees depending upon the composition and temperature of the surface [4]. RI is hindered by surfaces with an absence of unoccupied states which the excited He* electron can tunnel to [3]. Thus, typically RI+AN is supressed for non-metallic samples, while it dominates for high work function metals. Conversely, the AD process dominates for semiconducting, organic, and insulating surfaces, as well as surfaces with very low work functions [4, 10]. It is possible that a surface could have multiple unoccupied surface states, which leads to features being broadened in the RI+AN spectra [3, 4]. The resulting spectra are directly comparable between UPS and the AD components of MIES, where both show the same features but the relative sizes may be different [4].

Experimental

Cluster Source Depositions of Pt

A 99.9% pure Pt target was vaporized by pulsed laser vaporization. Prior to CS depositions, substrates were liquid N_2 cooled to 180 K, followed by a quick flash to 700 K to remove any

adventitious hydrocarbons. As the samples cooled after flash heating, deposition was started at 300 K and continued as the samples to 180 K. A RF quadrupole ion guide and bending unit were set to collect positively charged clusters. The beam passed through several differential pumping stages, before reaching a quadrupole mass filter which selected for a specific mass/charge ratio. Because multiply charged clusters have negligible intensity in the source distribution,[11, 12] this process selects a particular cluster size selection. Following size-selection, the clusters where guided into the UHV system, and passed through a 2 mm diameter aperture positioned 0.5 mm from the substrate surface, which produces cluster spots of ~2 mm in diameter. A retarding potential was used to achieve a deposition energy of ~1 eV/atom to prevent cluster damage or embedding [13]. Because the electron spectrometer analysis area was substantially larger than 2 mm, each CS-Pt_3 sample had 7 individual Pt_3 cluster spots deposited such that the spots did not overlap. Two CS-Pt_3/TiO_2 samples were prepared which had coverages of nominally 3 x 10^{13} atoms/cm^2 and 4.5 x 10^{13} atoms/cm^2 based on the measured neutralisation current during depositions. These values only include the cluster-deposited areas, not the blank substrate area in between. The ratio of cluster-covered area in the electron spectroscopy analysis area was ~0.22. A higher number of repeat samples for the CS-Pt_3 series would have been ideal for consistency with the other series, but in this case the number of samples was found to be sufficient for determining the UPS and MIES reference spectra due to the Pt_3 clusters.

XPS

Peak Fitting

CasaXPS was used to fit the peaks in the XPS spectra. Shirley backgrounds were subtracted from each spectrum before peak fitting. Individual reference peaks were typically fitted to the measured spectra using a convolution of Gaussian and Lorentzian line shapes. Peaks were fitted based on area, full width half maximum (FWHM) and peak location. The uncertainty in measured BEs is ± 0.2 eV, however in this study the presented BE's are averages from multiple samples and it was determined the weighted average standard deviation (taken to be the uncertainty) for cluster peak locations (for Ru 3d and Pt 4f) was ± 0.1 eV.

Every XPS spectrum featured C 1s peaks to some extent. For every sample peaks assigned to C-C or C-H were present at 285.0 eV, and C=O or C-O-C were present at 287.0 eV. A third carbon peak at 289.4 eV, assigned to O=C-O, was sometimes present but was typically removed by heat treatment and sputtering. These results are comparable to previously reported assignments for carbon contamination on SiO_2 substrates [14].

In the Ru 3d region, the adventitious C 1s peak overlaps with the Ru 3d doublet for clusters. To help with fitting the Ru 3d peak, a metallic Ru reference metal was analysed with XPS in our previous publication, and used as a fitting model for cluster Ru 3d spectra [15]. When comparing the $3d_{5/2}$ and $3d_{3/2}$ peaks, the peak separation was 4.17 eV, peak area ratio was 3:2, and FWHM ratio was 1:1.15.

Ru typically features asymmetrical line shapes for the 3d core electrons, and studies have been performed by Morgan [16] investigating the best way to fit this. The extent of asymmetry is dependent on the chemical nature of Ru as well as the resolution of the XPS instrument [16-18]. The line shapes published by Morgan were used as a starting point and were altered to best fit the line shape seen for the Ru clusters; LF(0.75,1.25,500,250) for Ru $3d_{5/2}$ and LF(0.8,1,500,250) for Ru $3d_{3/2}$. LF indicates Lorentzian asymmetric line shapes with tail damping.

For Pt_3 clusters the Pt 4f peaks were symmetrical. The Pt 4f region was fitted with 3 peaks, related to the Pt 4f doublet as well as an energy loss (E loss) peak in the same region which was also present for blank TiO_2. The fitting results for the blank TiO_2 were used as a template for the peak location and full width half maximum (FWHM) of the E loss peak when fitting results for samples with CS-Pt_3 present.

Calculation of Surface Coverage

Atomic concentrations as a percentage (At%) were determined using XPS. All the peaks associated with elements present on the surface were fitted and integrated to determine their peak area, and the areas were calibrated by dividing by XPS sensitivity factors found in the Handbook of X-ray Photoelectron Spectroscopy [19]. These were C 1s = 0.296, O 1s = 0.711, Ti 2p = 2.001, Ru 3d = 4.273, and Pt 4f = 5.575. The atomic ratios were determined by dividing the calibrated peak area for each element by the total calibrated peak area for all elements, and these were multiplied by 100% to determine the At%. The ratio of Ti^{3+} and Ti^{2+} peaks to the total summed Ti peak signals (Ti^{Defect}/Ti^{Total}, or Ti defect ratio) was calculated for each Defect-TiO_2 sample, and is used as a measurement for the level of defects in the titania.

The surface coverage of clusters was calculated for each sample and is presented in units of % ML, which is the percentage of the surface covered relative to a monolayer (ML). This calculation was done using a procedure similar to Eschen *et al.* [20], except for the difference that Eschen *et al.* used multiple XPS detection angles. This process solved for the surface coverage required to achieve the measured XPS At% for each cluster metal (Ru or Pt). The clusters were assumed to be present in only a single ML on the surface with negligible stacking of atoms and no mixing of cluster and substrate layers. The bulk interatomic distance for each metal was used to estimate the layer thickness for deposited Ru and Pt clusters, where Ru-Ru is 0.265 nm and Pt-Pt is 0.278 nm [21]. The contribution of individual atoms to the XPS spectra is reduced as the depth of the atom into the surface increases, which was also factored into the calculation by using the IMFP of electrons in TiO_2, 1.8 nm [22]. For Pt_3 measurements a scaling factor based on the ratio of the analysed surface covered by clusters was used in calculations.

Uncertainties

The relative uncertainty in At% varied depending on the size of the XPS peaks, and whether they overlapped with other peaks. Due to this, the uncertainty in At% for each peak of interest was

estimated by determining the largest range of peak areas which resulted in what was considered a reasonable peak fitting. The relative uncertainty for At% of deposited cluster peaks was ~4% for both Ru 3d and Pt 4f. For elements in the substrate, the relative uncertainty is ~1% for Ti^{4+} 2p and O 1s in TiO_2. The defects in TiO_2 spectra are present as Ti^{3+} and Ti^{2+} 2p peaks (these, when summed, are referred to as $Ti^{defects}$), and each has a relative uncertainty of ~15%.

A range of factors contribute to the uncertainty in surface coverage. These include errors in the calculated At% for the clusters, differences between atomic sensitivity factors in our detector setup and in the XPS handbook [19], and any inaccuracy in the IMFP of electrons in the substrate. Based mainly on the uncertainty of the IMFP, the absolute error in surface coverages was assumed to be ~100%. However, the relative error comparing between samples is based only on the cluster At% uncertainty and is ~4%. While the ~100% error can be considered high, the surface coverage estimation was intended only to give the scale of the surface coverage of clusters used in the experiments.

UPS and MIES

Determining Reference Spectra

To determine the reference spectrum due to deposited metal clusters, a blank TiO_2 spectrum was subtracted from each spectrum of cluster-loaded samples which were multiplied by linear scaling factors. The scaling factors were determined by minimising the differences between the resultant reference spectra for all samples in a series using the Excel Solver function. The resultant reference spectra from each sample were then averaged to determine an average reference spectrum for the sample series. In this process an assumption is made that the measured spectra are a linear combination of the substrate spectrum, and a spectrum related to the clusters. This assumes that the surface coverage does not affect the DOS of the clusters, which is reasonable considering the cluster-loaded surfaces were <20% ML, and similar assumptions for MIES spectra have been found to hold true for several systems [4]. The reference spectra were in some cases multiplied by a scaling factor for the figures for ease of comparison between spectra. For each sample series, weighting factors were determined for the contributions of the substrate and clusters to each measured spectrum, which provide evidence that the determined reference spectra are related to the cluster depositions. This is discussed further in the Supplementary Material.

Weighting Factors

Weighting factors for the substrate and cluster reference spectra from UPS and MIES were determined by linearly combining the substrate spectrum and the average reference spectrum. Weighting factors were determined using the Excel Solver function to minimise the sum of differences between the measured spectrum and the linear combination of reference spectra. For CS-Pt_3 the ratio of the substrate which was covered in clusters was factored into the reported weighting factors. The weighting factors were then normalised so that their sum was unity. The

uncertainty in weighting factors was estimated to be ± 0.05.

Results

XPS

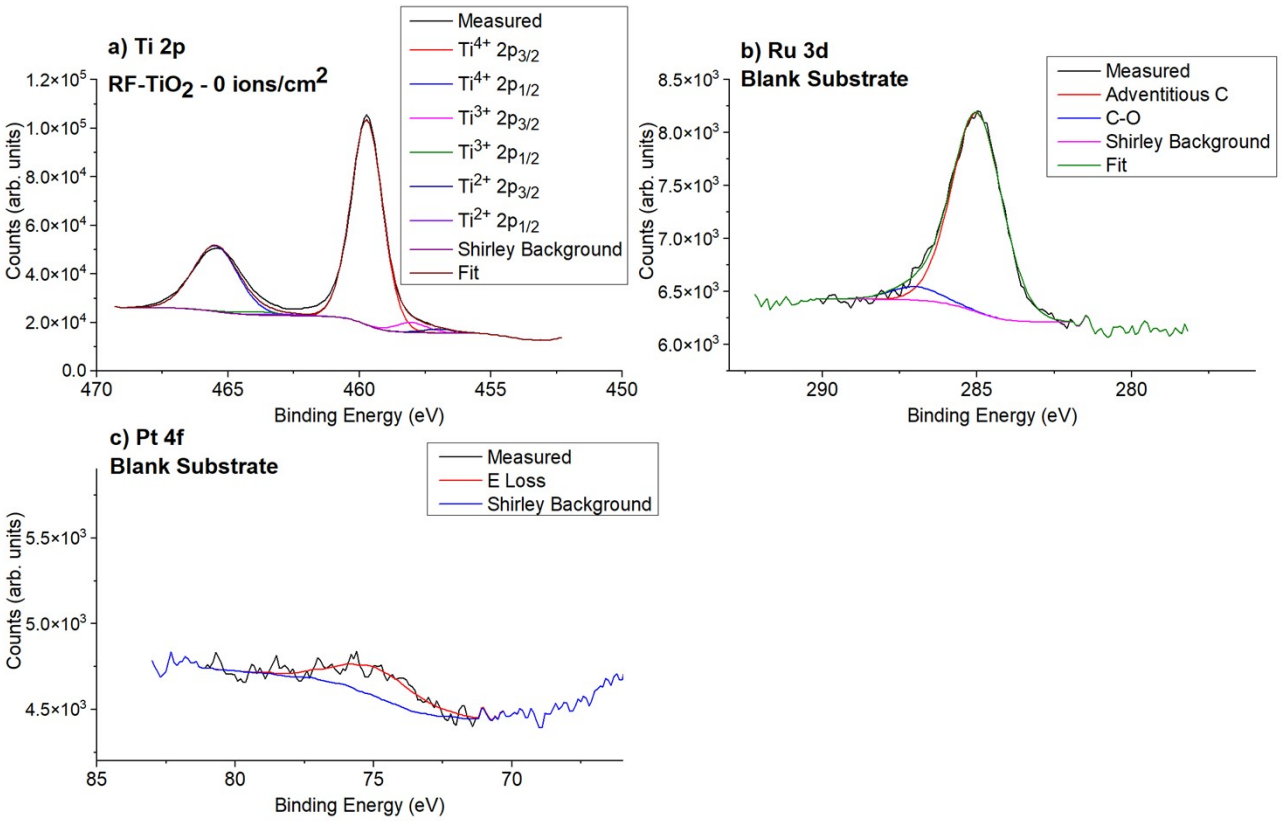

Figure S1: XPS peak fitting examples for blank samples with no clusters, which were used to assist with the fitting of the cluster-loaded samples. a) Ti 2p peak fitting for TiO_2, after heating to 723 K but prior to treatment with Ar^+ sputtering. b) Ru 3d/C 1s peak fitting for heated and sputtered TiO_2 prior to Ru cluster deposition. c) Pt 4f region fitting for heated and sputtered TiO_2 with no deposited Pt clusters.

Table S1: XPS results for each UPS/MIES sample after heating to 723 K. The At% was calculated for species of interest and is shown for Ti^{4+}, (Ti^{3+} + Ti^{2+}), and Ru or Pt. See the Methodology of the Supplementary Material for information on the relative uncertainties for At%.

Sample Series	Sample	Ti^{4+} At%	(Ti^{3+} + Ti^{2+}) At%	Ru or Pt At%
SD-Ru_3	SD-Blank	24.5	1.6	0
	SD-Ru_3-1	23.8	1.5	0.04
	SD-Ru_3-2	24.6	1.7	0.1
	SD-Ru_3-3	23.4	0.8	0.5
	SD-Ru_3-4	24.3	1.7	0.8
	SD-Ru_3-5	22.9	1.8	1.2
	SD-Ru_3-6	22.1	1.7	1.3
CVD-Ru_3	CVD-Blank	24.8	1.7	0
	CVD-Ru_3-1	23.9	2.0	0.2
	CVD-Ru_3-2	24.3	1.9	0.2
	CVD-Ru_3-3	23.0	2.2	0.4
	CVD-Ru_3-4	22.5	2.9	0.5
	CVD-Ru_3-5	23.7	2.2	0.6
CS-Pt_3	CS-Blank	23.2	1.9	0
	CS-Pt-1	22.5	1.8	0.07
	CS-Pt-2	22.4	2.2	0.09

UPS/MIES

Sample Series Weighting Factors

The weighting factors for the contributions of the blank substrate and the cluster reference spectra (or Ti defects) are shown in Figure S2. If the weighting factor for a spectrum related to clusters increases as the cluster surface coverage increases, this provides evidence that the determined reference spectrum is indeed related to the presence of the clusters.

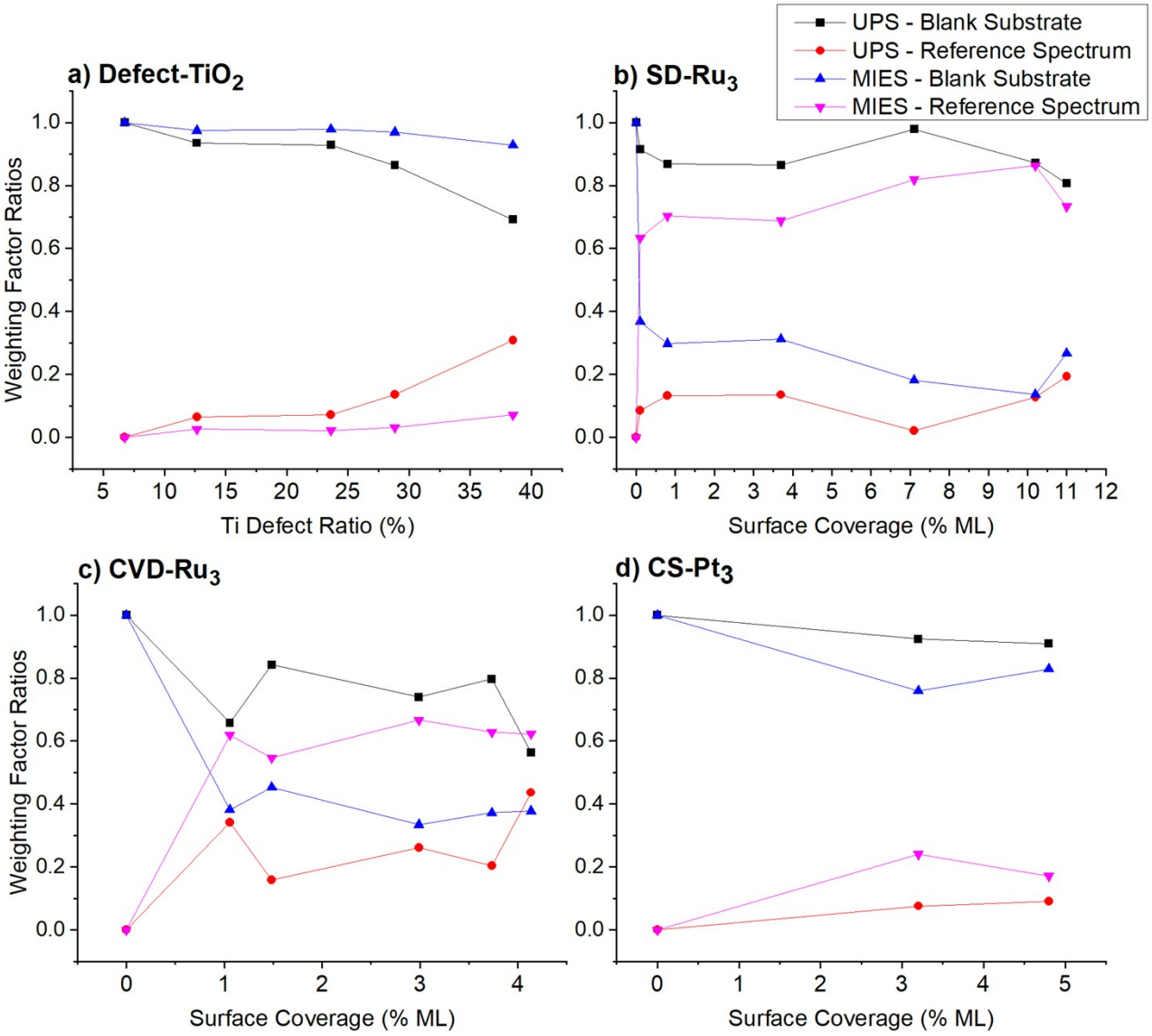

Figure S2: UPS/MIES weighting factors for the blank substrate spectrum and the calculated reference spectrum for each sample series. a) Defect-TiO_2. b) SD-Ru_3. c) CVD-Ru_3. d) CS-Pt_3. Weighting factors are plotted as a function of the Ti defect ratio (a) or cluster surface coverage (b-d) and have an uncertainty of ± 0.05.

The weighting factors for the Defect-TiO_2 reference spectra in both UPS and MIES increase approximately linearly with Ti^{Defect}/Ti^{Total} (Figure S2a). This provides evidence that the determined UPS/MIES reference spectra for Defect-TiO_2 are related to the Ar^+ sputter treatment, and thus most likely represent the UPS/MIES signal for surface defects.

The SD-Ru_3 UPS and MIES weighting factors increase approximately with Ru surface coverage (Figure S2b), providing evidence that the SD-Ru_3 reference spectra are related to the cluster depositions. The weighting factor for UPS increases with Ru surface coverage as expected, except for the 7.1% ML sample which was lower than the trend and appears to be an outlier. The MIES weighting factor for SD-Ru_3 increased from 0 to 0.63 for the lowest surface concentration compared to the blank, and then increases further with surface concentration. The large initial increase is most

likely due to the high surface sensitivity of MIES, where the surface layer is being changed more dramatically than for UPS due to the presence of the clusters.

The weighting factor for the UPS CVD-Ru_3 reference spectrum increases approximately linearly with Ru surface coverage (Figure S2c). The 1.1% ML measurement sample (1 minute CVD deposition) appears to be an outlier with a higher than expected weighting factor. The MIES weighting factor ratios for the CVD-Ru_3 reference spectrum increased from 0 to 0.62 for the lowest surface concentration, and then increases slightly further with surface coverage at higher concentrations, similar to what was seen for the MIES of SD-Ru_3. The increase in weighting factors is sufficient evidence that the determined UPS and MIES spectra for CVD-Ru_3 are related to the CVD depositions.

The CS-Pt_3 UPS reference spectrum weighting factor increases approximately linearly with Pt surface coverage, which provides evidence the CS-Pt_3 UPS reference spectrum is related to the deposition of Pt_3 clusters. The MIES weighting factor ratio for CS-Pt_3 increases from the blank (0% loading) to the 3.2% ML sample, but then decreases slightly for the 4.8% ML sample. However, this is deemed acceptable within the ± 0.05 uncertainty for the weighting factor ratios, and it is most likely the CS-Pt_3 MIES reference spectrum is also related to the deposition of Pt_3 clusters.

Table S2: Cluster surface coverages, determined from XPS measurements of as-deposited cluster samples at room temperature (see also Table 2) together with WF of all samples The error in WF is ± 0.1 eV.

Sample Series	Sample	Surface Coverage (% ML)	WF [eV]
SD-Ru_3	SD-Blank	0.0	4.8
	SD-Ru_3-1	0.1	4.6
	SD-Ru_3-2	0.8	4.5
	SD-Ru_3-3	3.7	4.8
	SD-Ru_3-4	7.1	4.4
	SD-Ru_3-5	10.2	4.5
	SD-Ru_3-6	11.0	4.3
CVD-Ru_3	CVD-Blank	0.0	4.8
	CVD-Ru_3-1	1.1	4.4
	CVD-Ru_3-2	1.5	4.7
	CVD-Ru_3-3	3.0	4.2
	CVD-Ru_3-4	3.7	4.2
	CVD-Ru_3-5	4.1	4.6
CS-Pt_3	CS-Blank	0.0	4.1
	CS-Pt-1	3.2	4.0
	CS-Pt-2	4.8	4.1

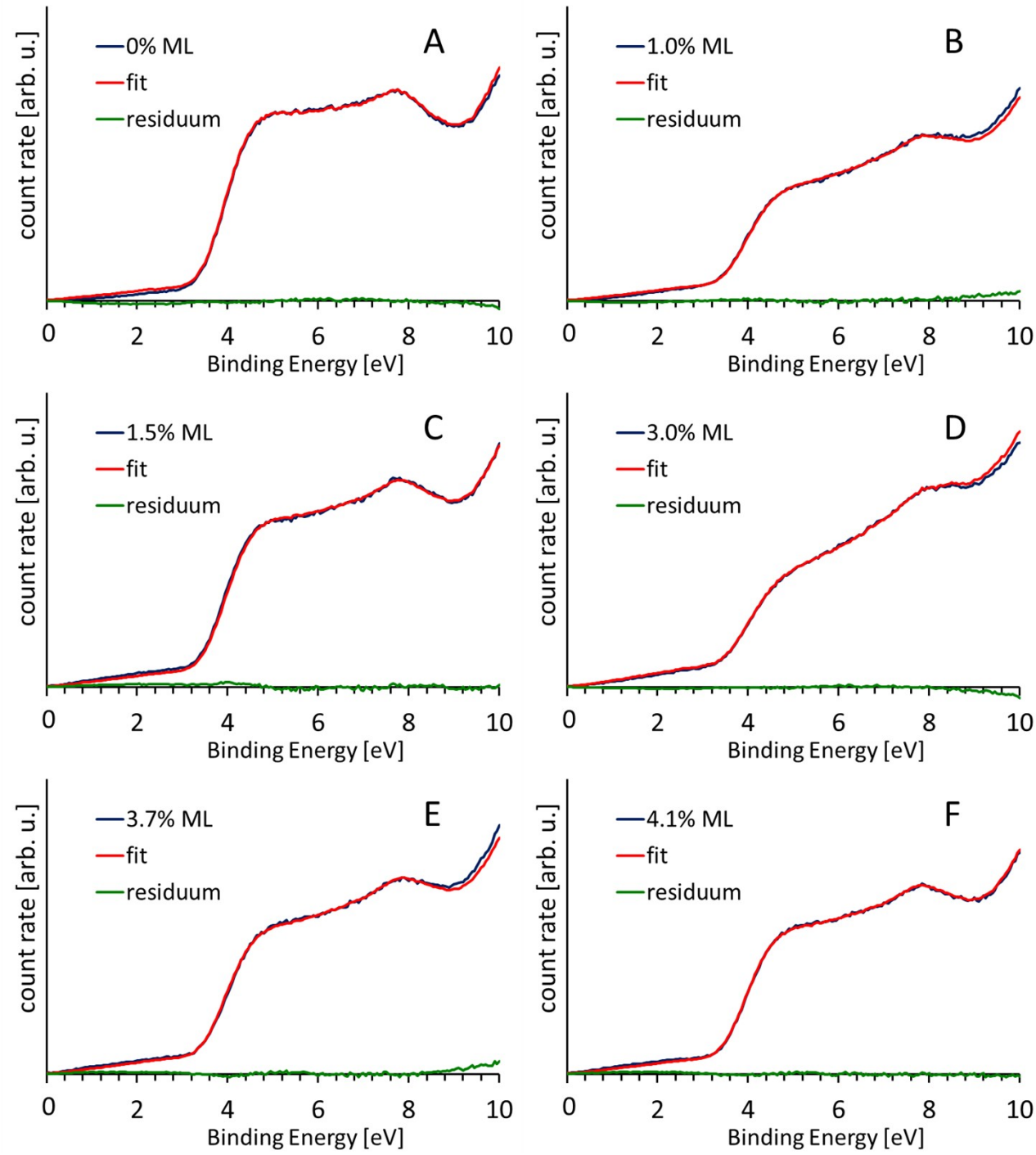

Figure S3: fits of the UPS results for the CVD-Ru3 sample series after heating for the loadings investigated (A – F).

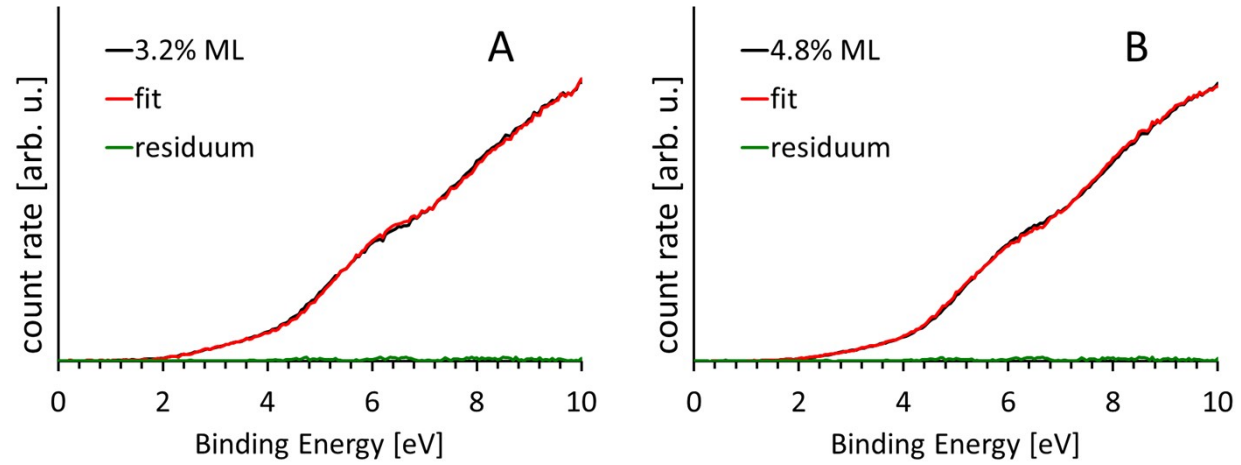

Figure S4: fits of the MIES results for the CS-Pt3 sample series after heating for the loadings investigated (A – B).

Metallic Reference Sample

A UPS/MIES measurement was performed on a 99.9% pure sample of bulk, metallic Ru, and is shown in Figure S3. The sample was treated by heating to 1073 K for 10 minutes and sputtering with 3 keV Ar^+ ions for 1 hour to remove the surface Ru oxide layer and any hydrocarbon contamination, which was confirmed by XPS.

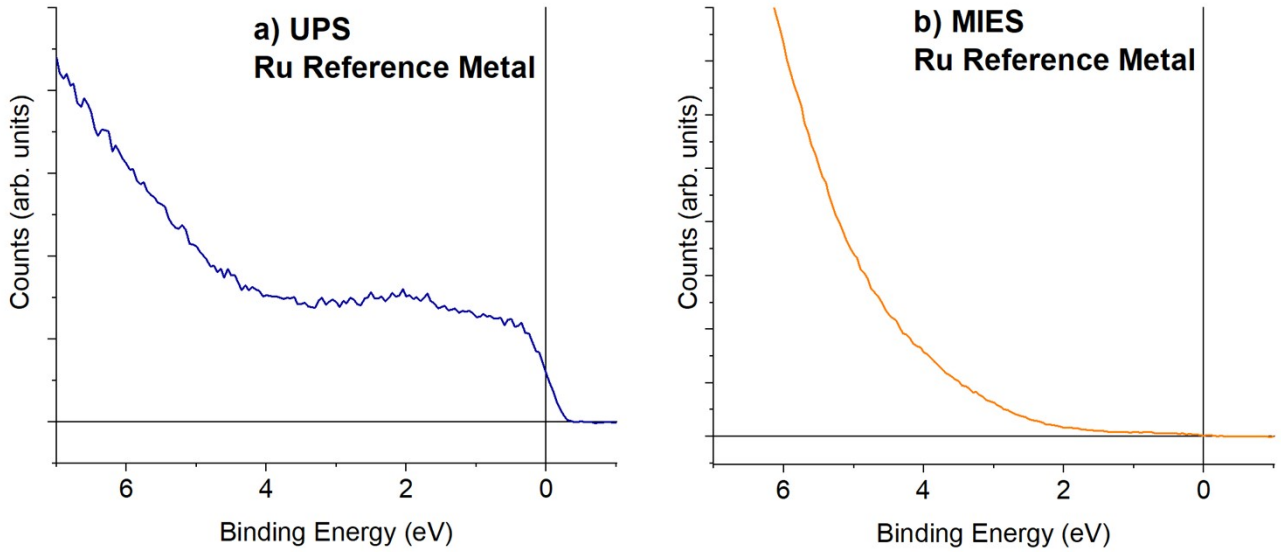

Figure S5: Valence electron spectra for bulk, metallic Ru. a) UPS results, b) MIES results.

The UPS spectrum for metallic Ru (Figure S5a) shows an onset at the Fermi level, which is expected for a bulk metallic sample [23-27], and has features present at 0.3 eV and 2.0 eV. The MIES spectrum (Figure S5b) has no distinct features, and features a broad, increasing background. This is because the MIES spectrum was the result of Auger neutralisation (AN) and resonance ionisation (RI), which is typical for metallic samples and results in a spectrum which is broadened compared to

the true valence DOS [4]. Note that the BE axis of Figure S5b does not strictly show the true BE with regards to the DOS due to this broadening, but the BE axis was still used for consistency.

A bulk, high purity metallic Pt reference material was not available for analysis with UPS and MIES in this study. However, a reference UPS measurement of the Pt(111) surface is available in a study by Crowell *et al*. [28], where the onset of the spectrum was at the fermi level as per the Ru UPS reference above, and there were 3 distinct d-band peaks between 0 and 6 eV. No previous Pt reference measurement using MIES has been published, but it is expected the spectrum would look similar to the Ru MIES spectrum above, because the metallic nature of the surface would promote AN+RI de-excitation.

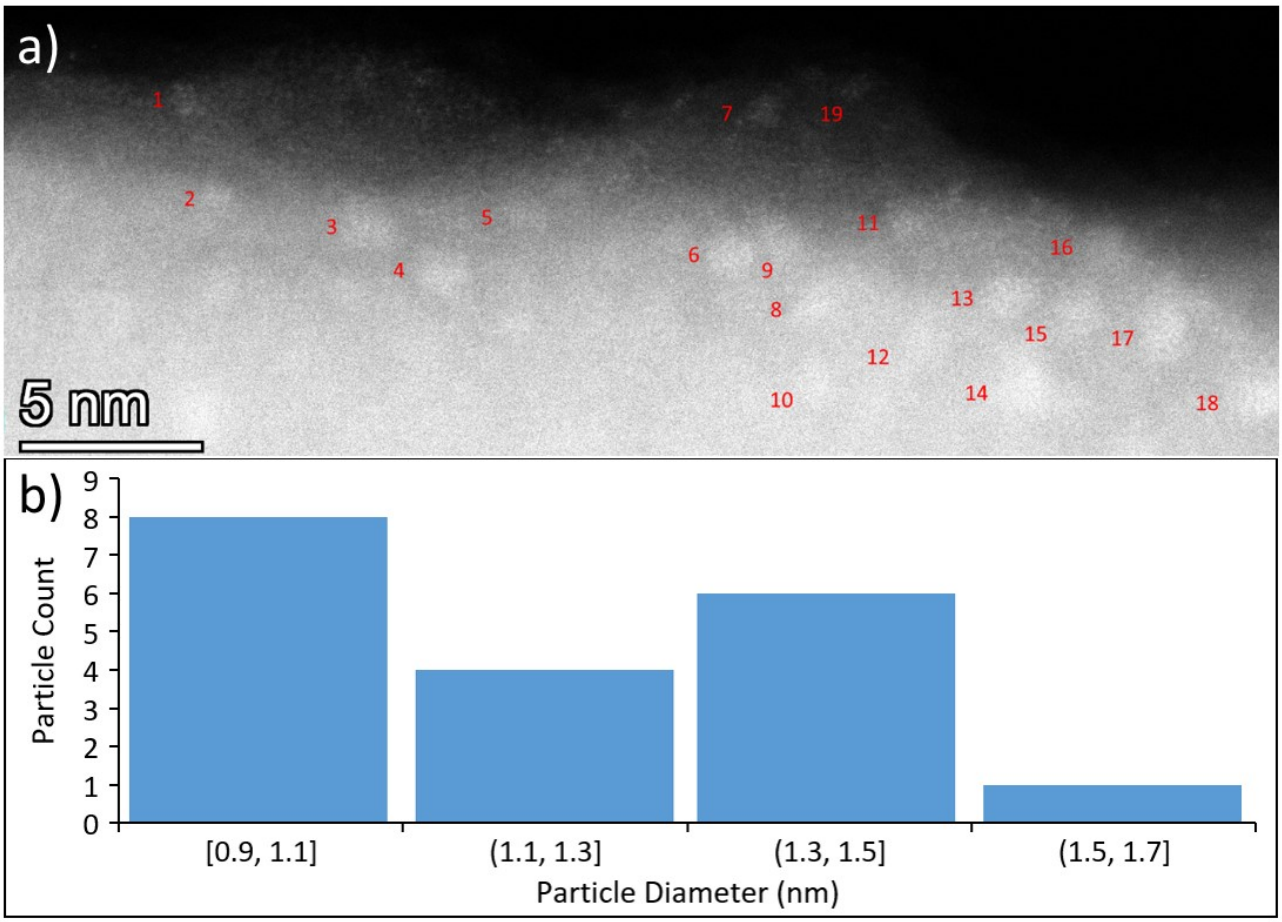

Figure S6: STEM of CVD-$Ru_3(CO)_{12}$/HDS-RF-TiO_2, showing side-on perspective of sample. a) STEM image with numbered, encapsulated Ru clusters (cluster sizes shown individually in Table S5). b) Distribution of particle diameters for encapsulated Ru clusters. Reproduced with permission from reference [15].

References

[1] J. Rowe, H. Ibach, Surface and bulk contributions to ultraviolet photoemission spectra of silicon,

Phys. Rev. Lett. 32 (1974) 421.
[2] M. Seah, W. Dench, Quantitative electron spectroscopy of surfaces: a standard data base for electron inelastic mean free paths in solids, Surf. Interface Anal. 1 (1979) 2-11.
[3] Y. Harada, S. Masuda, H. Ozaki, Electron spectroscopy using metastable atoms as probes for solid surfaces, Chem. Rev. 97 (1997) 1897-1952.
[4] H. Morgner, The characterization of liquid and solid surfaces with metastable helium atoms, Adv. At. Mol. Opt. Phys. 42 (2000) 387-488.
[5] B.A. Chambers, C.J. Shearer, L. Yu, C.T. Gibson, G.G. Andersson, Measuring the density of states of the inner and outer wall of double-walled carbon nanotubes, Nanomaterials 8 (2018) 448.
[6] G. Krishnan, H.S. Al Qahtani, J. Li, Y. Yin, N. Eom, V.B. Golovko, G.F. Metha, G.G. Andersson, Investigation of Ligand-Stabilized Gold Clusters on Defect-Rich Titania, J. Phys. Chem. C 121 (2017) 28007-28016.
[7] G. Krishnan, N. Eom, R.M. Kirk, V.B. Golovko, G.F. Metha, G.G. Andersson, Investigation of Phosphine Ligand Protected Au13 Clusters on Defect Rich Titania, J. Phys. Chem. C 123 (2019) 6642−6649.
[8] G.G. Andersson, V.B. Golovko, J.F. Alvino, T. Bennett, O. Wrede, S.M. Mejia, H.S. Al Qahtani, R. Adnan, N. Gunby, D.P. Anderson, Phosphine-stabilised Au9 clusters interacting with titania and silica surfaces: The first evidence for the density of states signature of the support-immobilised cluster, J. Chem. Phys. 141 (2014) 014702.
[9] H.D. Hagstrum, Excited-Atom Deexcitation Spectroscopy using Incident Ions, Phys. Rev. Lett. 43 (1979) 1050.
[10] B. Heinz, H. Morgner, A metastable induced electron spectroscopy study of graphite: The k-vector dependence of the ionization probability, Surf. Sci. 405 (1998) 104-111.
[11] H. Haberland, Mall, M., Moseler, M., Qiang, Y., Reiners, T., and Thurner, Y., Filling of micron-sized contact holes with copper by energetic cluster impact, J. Vac. Sci. Technol. A 12 (1994) 2925-2930.
[12] H. Haberland, Karrais, M., Mall, M., and Thurner, Y., Thin films from energetic cluster impact: A feasibility study, J. Vac. Sci. Technol. A 10 (1992) 3266-3271.
[13] V.N. Popok, I. Barke, E.E.B. Campbell, K.-H. Meiwes-Broer, Cluster–surface interaction: From soft landing to implantation, Surf. Sci. Rep. 66 (2011) 347-377.
[14] E.L. Strein, D. Allred, Eliminating carbon contamination on oxidized Si surfaces using a VUV excimer lamp, Thin Solid Films 517 (2008) 1011-1015.
[15] L. Howard-Fabretto, T.J. Gorey, G. Li, S. Tesana, G.F. Metha, S.L. Anderson, G.G. Andersson, The interaction of size-selected Ru3 clusters with RF-deposited TiO2: probing Ru-CO binding sites with CO-Temperature Programmed Desorption, Nanoscale Advances (2021).
[16] D.J. Morgan, Resolving ruthenium: XPS studies of common ruthenium materials, Surf. Interface Anal. 47 (2015) 1072-1079.
[17] Y.J. Kim, Y. Gao, S.A. Chambers, Core-level X-ray photoelectron spectra and X-ray photoelectron diffraction of RuO2 (110) grown by molecular beam epitaxy on TiO2 (110), Appl. Surf. Sci. 120 (1997) 250-260.
[18] J. Riga, C. Tenret-Noel, J.-J. Pireaux, R. Caudano, J. Verbist, Y. Gobillon, Electronic structure of rutile oxides TiO2, RuO2 and IrO2 studied by X-ray photoelectron spectroscopy, Phys. Scr. 16 (1977) 351.
[19] J. Chastain, Handbook of X-ray photoelectron spectroscopy, Perkin-Elmer Corporation, Minnesota, USA, 1992, pp. 221.
[20] F. Eschen, M. Heyerhoff, H. Morgner, J. Vogt, The concentration-depth profile at the surface of a solution of tetrabutylammonium iodide in formamide, based on angle-resolved photoelectron spectroscopy, J. Phys. Condens. Matter 7 (1995) 1961.
[21] L. Sutton, Tables of interatomic distances and configuration in molecules and ions, Chemical Society1965.
[22] G. Fuentes, E. Elizalde, F. Yubero, J. Sanz, Electron inelastic mean free path for Ti, TiC, TiN and TiO2 as determined by quantitative reflection electron energy-loss spectroscopy, Surf. Interface Anal. 33 (2002) 230-237.
[23] C. Mead, W. Spitzer, Fermi level position at semiconductor surfaces, Phys. Rev. Lett. 10 (1963) 471.
[24] G. Wertheim, S. DiCenzo, Cluster growth and core-electron binding energies in supported metal clusters, Phys. Rev. B 37 (1988) 844.

[25] S. DiCenzo, G. Wertheim, Photoelectron spectroscopy of supported metal clusters, Solid State Phys. 11 (1985) 203.
[26] W. Eberhardt, P. Fayet, D. Cox, Z. Fu, A. Kaldor, R. Sherwood, D. Sondericker, Photoemission from mass-selected monodispersed Pt clusters, Phys. Rev. Lett. 64 (1990) 780.
[27] D.J. Alberas, J. Kiss, Z.-M. Liu, J.M. White, Surface chemistry of hydrazine on Pt (111), Surf. Sci. 278 (1992) 51-61.
[28] J. Crowell, E. Garfunkel, G. Somorjai, The coadsorption of potassium and CO on the Pt (111) crystal surface: A TDS, HREELS and UPS study, Surf. Sci. 121 (1982) 303-320.